Two-dimensional temperature feedback control strategy for thermal ablation of biological tissue

Leonardo Bianchi
Department of Mechanical Engineering, Politecnico di Milano
Milan, Italy
leonardo.bianchi@polimi.it

Annalisa Orrico
Department of Mechanical Engineering, Politecnico di Milano
Milan, Italy
annalisa.orrico@mail.polimi.it

Sanzhar Korganbayev
Department of Mechanical Engineering, Politecnico di Milano
Milan, Italy
sanzhar.korganbayev@polimi.it

Martina De Landro
Department of Mechanical Engineering, Politecnico di Milano
Milan, Italy
martina.delandro@polimi.it

Paola Saccomandi
Department of Mechanical Engineering, Politecnico di Milano
Milan, Italy
paola.saccomandi@polimi.it

2021 IEEE International Workshop on Metrology for Industry 4.0 & IoT (MetroInd4.0&IoT) | 978-1-6654-1980-2/21/$31.00 ©2021 IEEE | DOI: 10.1109/METROIND4.0IOT51437.2021.9488457

***Abstract*—During thermal ablative procedures, the control of the thermal doses delivered to the target area is an essential factor for inducing the required thermal effect while preventing undesired damage to the surrounding healthy tissue. In this study, we propose a two-dimensional temperature control strategy exerted through millimeter-scale temperature measurements during superficial laser ablation (LA) of *ex vivo* porcine hepatic tissue. A theoretical model was developed as a pre-planning tool to accurately predict the laser-induced temperature increase during the controlled ablation, the temperature evolution, the two-dimensional thermal distribution, and attained tissue injury after superficial ablation. The temperature increase in the target area was controlled based upon the selection of biologically relevant temperature thresholds, i.e., 43 °C and 55 °C, and the maintenance of these thermal values at specific distances from the center of the laser beam. The experimental outcomes well validated the implemented theoretical model (e.g., a maximum difference of predicted and measured extension of superficial thermal damage of ~0.5 mm). Therefore, the model resulted well suited for evaluating the pre-treatment setting parameters of the control strategy and designing the optimal characteristics of the sensing system. The attained results demonstrate the efficacy of the two-dimensional LA strategy to ensure the confinement of the desired temperatures within the selected region.**

Keywords— feedback system, closed-loop temperature control, real-time monitoring, thermal ablation, laser, liver, fiber Bragg grating sensors

I. Introduction

Minimally invasive thermal ablation procedures have aroused the interest of the biomedical community thanks to several benefits, over conventional methods, for the treatment of tumorous tissues [1]. For instance, the minimized operative trauma and shortened recovery time associated with these techniques may provide beneficial effects compared to traditional surgical approaches [2]. Among the thermal procedures that have been developed on account of technological advancements, laser ablation (LA) is gaining recognition due to the possibility to deliver the laser light through magnetic resonance- and computed tomography-compatible optical fibers and to be combined with endoscopic ultrasound guidance [3]. The physical phenomenon underlying LA is the photothermal conversion of near-infrared (NIR) light absorbed by biological components. The resulting temperature increase entails different responses on the target tissue depending on the reached temperatures and the time these temperatures are maintained. Temperatures ranging from 42 °C to 45 °C demonstrated to increase the cells' susceptibility to injury [4], while at temperatures higher than 50 °C coagulative necrosis can be observed [5].

The principal hurdle still preventing the widespread employment of LA in the clinical routine is related to the complexity to the deliver the thermal dose to the target zone without compromising the integrity of the surrounding tissue. Indeed, the procedure is typically carried out without real-time monitoring and feedback control able to adapt the energy delivery according to the tissue thermal outcome. Several studies have therefore focused on different strategies to improve the therapeutic effectiveness of the procedure: *i*) the increase of the LA selectivity based on the enhancement of the laser absorption only in the desired neoplastic site thanks to tumor-loaded photosensitizers [6], *ii*) the use of predictive tools to optimize the setting parameters prior to the treatment [7], and *iii*) the development of technological systems to modulate the laser irradiance based on a closed-loop approach which considers the tissue's thermal behavior. Concerning the latter strategy, the feasibility of temperature controlling approaches implemented based upon fiber Bragg grating (FBG) sensors has been recently assessed by our group [8], [9]. Compared to the state-of-the-art temperature controlling methods, which typically exert the control based on single-point measurement systems (i.e., thermocouples [10], [11], or thermistors [12], [13]), FBGs take advantage of the multiplexing capabilities, the ability to measure the temperature in multiple points, the immunity to electromagnetic fields, and the possibility to reconstruct spatially resolved two-dimensional thermal maps within the irradiated tissue [14], [15]. However, to set up a complete treatment strategy, the different parameters of the FBG-based

This project has received funding from the European Research Council (ERC) under the European Union's Horizon 2020 research and innovation programme (Grant agreement No. 759159).

978-1-6654-1980-2/21/$31.00 ©2021 IEEE

Authorized licensed use limited to: Politecnico di Milano. Downloaded on July 29,2021 at 07:51:18 UTC from IEEE Xplore. Restrictions apply.

controlling system should be theoretically investigated before experiments to analyze the best procedural settings. From here, the necessity to implement also reliable simulation-based tools of the controlled procedure.

In this study, we propose a combined approach based on the development of a theoretical model for the pre-planning of two-dimensional temperature feedback-controlled superficial LA and on its experimental validation. The effects of influential parameters selected to exert the controlled treatment (i.e., the temperature thresholds to be maintained within specified areas of the tissue surface) were evaluated in terms of attained temperature trends, two-dimensional thermal distribution, and final thermal damage.

II. Materials and Methods

A. Theoretical model of temperature controlled-LA

We implemented a computational model of the laser-induced thermal response of *ex vivo* liver tissue undergoing temperature-controlled LA, which served as a pre-planning platform. According to the empirical evaluation, three optical fibers inscribed with the FBG arrays were modeled on the surface of a cylinder simulating the liver tissue sample (Fig. 1.a). The following materials and specifications were considered for each optical fiber: fiber coating in polyimide material (radius of 62. 5 µm) and cladding in silica glass (radius of 77. 5 µm). The physical properties of both the hepatic tissue and the fiber optic sensors were considered in the model [16].

A tetrahedral mesh, with maximum and minimum sizes of 1 mm and 0.005 mm, respectively, was utilized to discretize the geometry domain (Fig. 1.b). The governing equations were solved by Finite Element Method (FEM) employing COMSOL Multiphysics software (COMSOL, Inc., Burlington, MA, USA). The simulation outcomes were used to predict the results of the control approach, described in section C, in terms of temperature evolution, two-dimensional thermal maps, and attained tissue damage, during superficial ablation.

The interaction of the NIR radiation with biological media was modeled accounting on the Beer-Lambert law. Hence, the heat source term Q_{laser}(W·m^{-3}), ascribed to electromagnetic monochromatic radiation interacting with tissue, was defined as [17]:

$$Q_{laser} = \mu_{eff} \cdot I \cdot e^{-\mu_{eff} \cdot z} \tag{1}$$

in which μ_{eff} (m^{-1}) is the effective attenuation coefficient, I (W·m^{-2}) represents the laser irradiance, and z (m) is the axial tissue depth. The μ_{eff}, expressed in the (1), was utilized in order to consider both the absorption and scattering phenomena occurring in NIR irradiated-biological soft tissues, typically defined as turbid media [18].

The tissue's thermal behavior during the photothermal treatment was theoretically predicted by means of the Pennes' bioheat equation [19]–[21]:

$$\rho \cdot c \frac{\partial T}{\partial t} = \nabla(k \nabla T) + Q_{laser} \tag{2}$$

being ρ (kg·m^{-3}) the tissue density, c (J·kg^{-1}·K^{-1}) is the tissue specific heat, k (W·m^{-1}·K^{-1}) refers to the thermal conductivity of tissue, and T (K) is the tissue temperature. The contributions of perfusion and metabolic heat were considered null since LA was performed on *ex vivo* porcine tissue. Additionally, the attained thermal damage was estimated based on the first-order Arrhenius equation [22], [23]:

$$\Omega(t) = A_f \cdot \int_0^{\tau} exp\left(-\frac{E_a}{R \cdot T(t)}\right) dt \tag{3}$$

where $\Omega(t)$ is the thermal damage, A_f (s^{-1}) is the frequency factor, E_a (J·mol^{-1}) is the denaturation activation energy, R (J·mol^{-1}·K) is the universal gas constant, and τ (s) is the ablation time. The kinetic coefficients associated with morphological variations in tissue due to thermally induced protein denaturation were selected from [24].

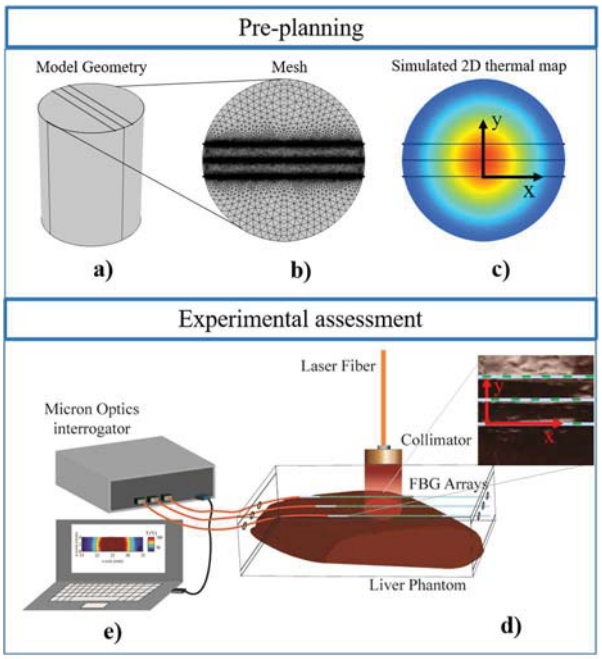

Fig. 1. Schematics of the two-dimensional (2D) temperature feedback control strategy for contactless ablation: (a) geometry of the computational model, (b) tetrahedral mesh of the model, (c) simulated 2D thermal map of the tissue surface, (d) experimental set-up with a close-up of the fiber positioning on the surface of the liver specimen, (e) computer showing the real-time temperature distribution experimentally assessed and utilized for the model validation.

B. Experimental evaluation

Laser irradiation was performed in a contactless modality with a diode laser with a characteristic wavelength of 808 nm. The NIR light was delivered through a quartz optical fiber (400 µm-diameter, numerical aperture of 0.22) coupled with a collimator (OZ Optics Ltd., Ottawa, ON, Canada) to control the beam diameter (i.e., 1 cm). The exposure time was 90 s. To attain high-resolved temperature measurements to monitor and regulate the laser treatment, three single-mode optical fibers SM1500(9/125)P (Fibercore Ltd., Southampton, UK), each embedding 40 FBG sensors, were utilized. The coating of the fiber was in highly resistant polyimide material and each FBG sensor was characterized by a grating length of 1.19 mm. Details of the sensors fabrication are provided in [15]. The optical fibers were positioned on the tissue surface at a distance of 2 mm along the y-axis (Fig. 1.d). The accurate positioning was facilitated by employing a custom-made box with apertures located at a 2 mm distance

Authorized licensed use limited to: Politecnico di Milano. Downloaded on July 29,2021 at 07:51:18 UTC from IEEE Xplore. Restrictions apply.

from each other in correspondence with the entrance of the fibers. The interrogation unit (Micron Optics si255) was used to illuminate the FBG sensors with broadband light and to detect the wavelength shift of the spectrum due to temperature change. Finally, a program in LabVIEW was implemented to receive the spectral data, convert them into temperature values and perform the temperature control as described in the following section.

C. Temperature controlling approach

The temperature control strategy herein employed, both in the simulated and experimental studies, relies on an ON-OFF approach, in which the laser power (P) is automatically set either on the ON-state (P = 5 W) or on the OFF-state (P = 0 W). The power regulation is performed according to the temperature values attained at specific locations of the tissue surface, during the contactless LA procedure. In the experimental evaluation, the real-time control is based on the temperature values registered by the FBG sensors embedded in the three optical fibers located at a distance of 2 mm from each other, positioned on the tissue surface (Fig. 1.d) [15]. Firstly, laser irradiation up to <35 °C is executed to attain the thermal profiles associated with each fiber and align them according to the centroid method, as described in [15]. Subsequently, a linear interpolation of the temperature values obtained by the FBGs over time is performed to reconstruct a complete two-dimensional thermal map. The temperature in a target area is then controlled based upon the selection of temperature thresholds (T_{th}) and the execution of the ON-OFF control for the maintenance of these thermal values (T_r) at specific distances from the center of the laser beam (i.e., on the circumference centered at the center of the laser beam and having a radius equal to r). The laser is in the ON-state when $T_r \leq T_{th}$ or in the OFF-state in case of $T_r > T_{th}$. Concerning the simulated pre-planning model, the control is performed in the same modality, although the alignment of the thermal profile is not required. Indeed, a two-dimensional map is already obtained by simulating the temperature reached at every point of the tissue surface. The optical fibers were simulated in order to consider also their physical properties on the final thermal outcome.

III. Results and Discussion

Two temperature thresholds T_{th}, i.e., 43 °C and 55 °C, were selected in the present study. Hence, the maintenance of these thermal values at specific distances from the center of the laser beam (i.e., r = 6 mm and r = 2 mm) was theoretically assessed and experimentally validated. The choice to implement the feedback control at these thresholds refers to the biological relevance of the selected temperatures. Particularly, within the temperature range comprised between 42 °C and 45 °C, moderate hyperthermia can enhance the

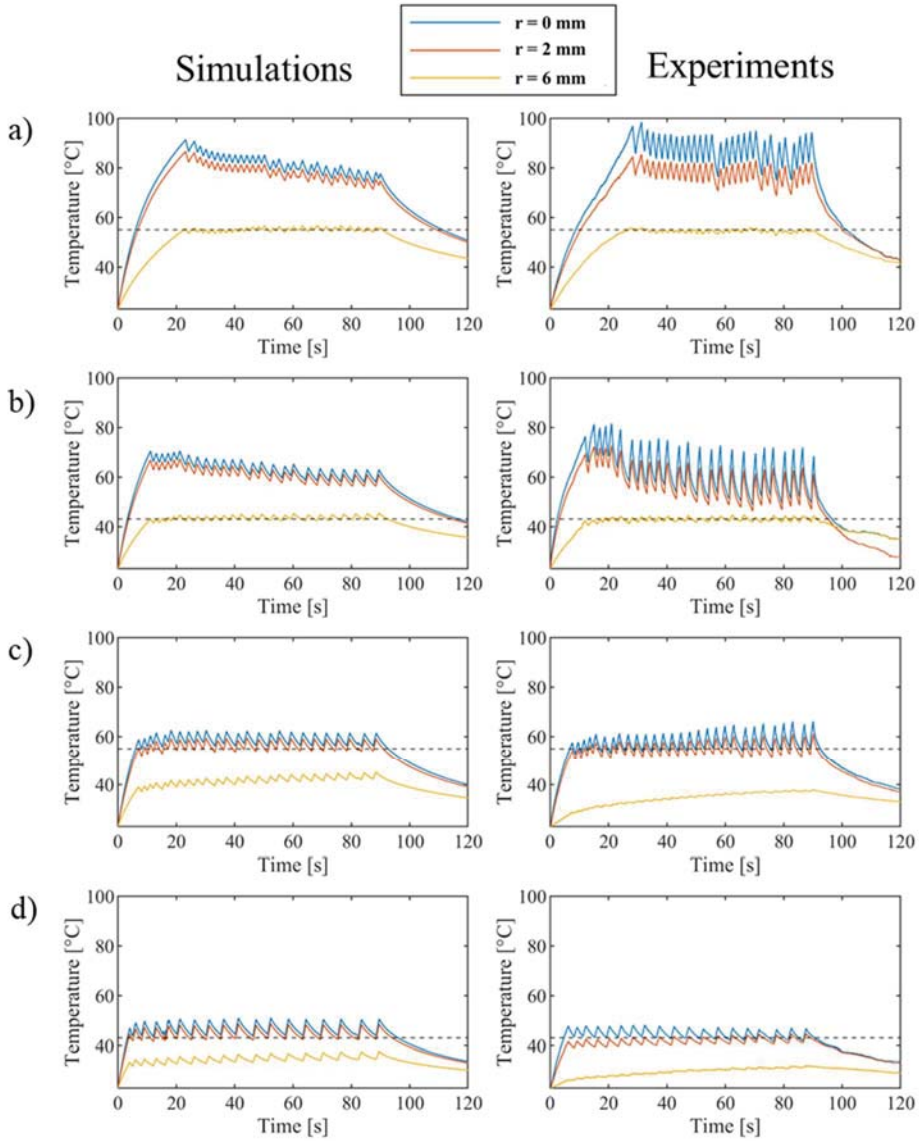

Fig. 2. Temperature trends over time attained for simulation (left column) and experiments (right column) in case of: (a) r = 6 mm, T_{th} = 55 °C, (b) r = 6 mm, T_{th} = 43 °C, (c) r = 2 mm, T_{th} = 55 °C, (d) r = 2 mm, T_{th} = 43 °C.

Authorized licensed use limited to: Politecnico di Milano. Downloaded on July 29,2021 at 07:51:18 UTC from IEEE Xplore. Restrictions apply.

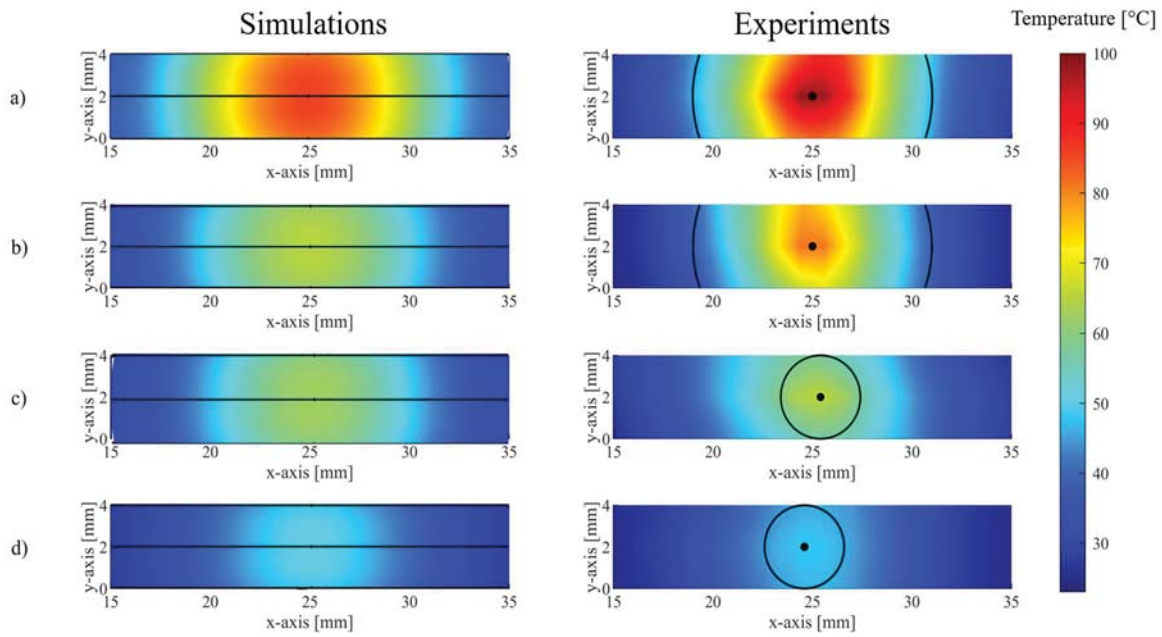

Fig. 3. Two-dimensional thermal maps attained for simulation (left column) and experiments (right column) in case of: (a) r = 6 mm, T_{th} = 55 °C, (b) r = 6 mm, T_{th} = 43 °C, (c) r = 2 mm, T_{th} = 55 °C, (d) r = 2 mm, T_{th} = 43 °C.

tissue selectivity [4], while between 50 °C and 55 °C irreversible cell damage can occur.

Furthermore, over these thresholds, e.g., thermal values higher than 60 °C, instantaneous thermal injury is observable [5].

Concerning the different control cases, Fig. 2 shows the temperature trends over time attained in case of simulated LA (left column) and the experimental measurements (right column). For all the graphs, the temperature values in correspondence of different distances from the center of the laser beam (i.e., 0 mm, 2 mm, and 6 mm) are reported. In all the investigated cases, the temperature at the selected distance was maintained close to the $T_{th,}$ and the simulation well approximated the empirical results. For both the estimated and experimentally registered temperature trends a sawtooth-like profile is observed from the start of the controlling phase, i.e., the first time T_r equals T_{th}. This is due to the repeated change of the delivered laser power between the ON-state and the OFF-state to regulate the thermal outcome within the selected tissue margins.

The simulated temperature evolution well predicted the experimental results in terms of time needed to activate the control for the first time (t_{act}). That is the time elapsed between the instant in which the laser is turned on at the beginning of the irradiation and the instant in which P is automatically set to 0 W for the first time. Regarding the simulated trends, for r = 6 mm, the values of t_{act} resulted equal to 23.3 s and 11.0 s, respectively for T_{th} = 55 °C (Fig. 2.a) and T_{th} = 43 °C (Fig. 2.b). The corresponding values for the experimental trends were 28.3 s and 12.0 s. Furthermore, in case of r = 2 mm, and for T_{th}= 55 °C and T_{th} = 43 °C, t_{act} was 7.0 s (Fig. 2.c) and 4.2 s (Fig. 2.d), in the simulation. While the experimental results showed t_{act} equal to 7.6 s and 6.2 s, respectively for T_{th} = 55 °C and T_{th} = 43 °C.

Overall, the simulation was able to estimate the control activation with a maximum discrepancy of 5 s from the experiments. It is worth noticing that both simulated and bench tests indicated that the control performed at r = 2 mm is characterized by lower values of t_{act} compared to the control at r = 6 mm. Moreover, considering the same control distances, the higher the T_{th} the higher the time needed to activate the control.

Regarding the thermal distribution associated to the different case-studies, Fig. 3 depicts the two-dimensional thermal maps attained for the computationally modeled LA (left column) and the experimental assessment (right column). In the left column, the positions of the optical fibers are illustrated (i.e., 0 mm, 2 mm, and 4 mm along the y-axis), whereas in the right column the arches of the circumferences of different controlled areas are represented. The FBG sensors thanks to their quasi-distributed characteristics [15] permitted to reconstruct a real-time spatially-resolved temperature map that can be compared to the heat distribution predicted by the developed model. The thermal distributions refer to the instant of time in which the maximum temperatures were registered. As it is possible to observe, the simulation was capable to well describe the tissue's thermal behavior. In each case, the maximum temperature was found in correspondence to the laser beam axis, at the center of the controlled superficial zone. For r = 6 mm and T_{th} = 55 °C, the maximum temperatures obtained during the photothermal ablation were 91.3 °C and 98.5 °C, for simulation and experiments, correspondingly (Fig. 3.a). At the same control distance, but for T_{th} = 43 °C, the attained maximum values were equal to 70.5 °C for simulated LA while 81.6 °C for experiments (Fig. 3.b). Considering the controlled ablation performed along the circumference having r = 2 mm, the model predicted a maximum temperature of 62.4 °C and 51.8 °C, for T_{th} equal to 55 °C and 43 °C, respectively. The corresponding measured values were 66.2 °C and 48.2 °C (Figs. 3.c and 3.d). As observable, considering the same distance at which the control was performed, the selection of a lower T_{th} induced lower maximum temperatures. Moreover, the choice of the distance from the center of the laser beam

Authorized licensed use limited to: Politecnico di Milano. Downloaded on July 29,2021 at 07:51:18 UTC from IEEE Xplore. Restrictions apply.

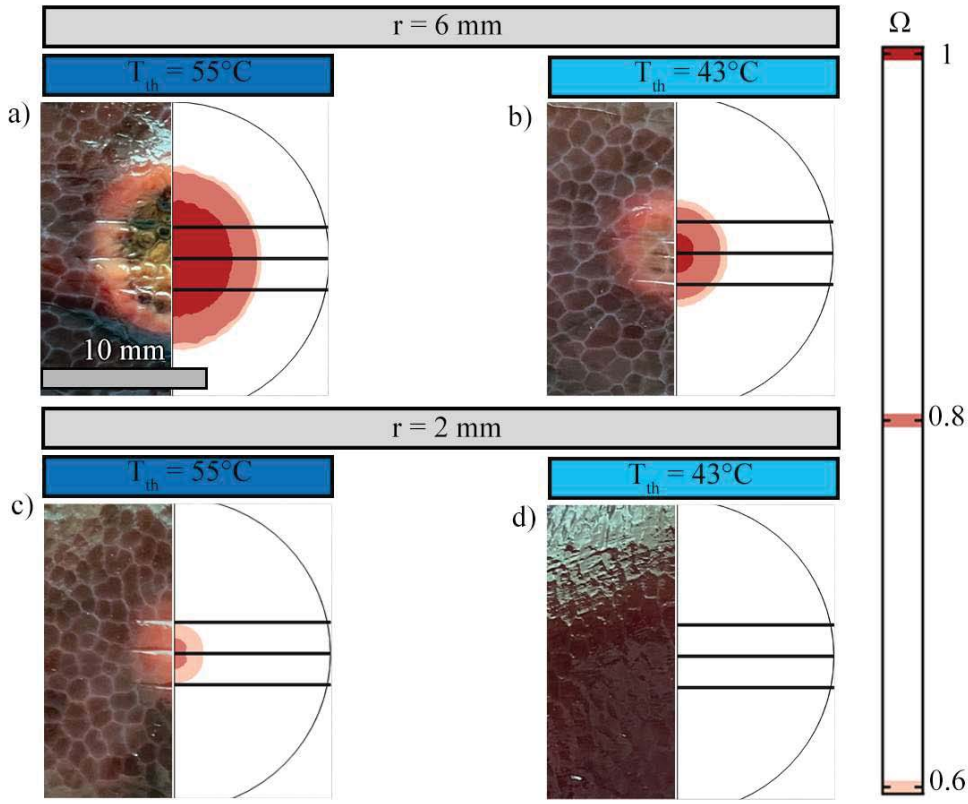

Fig 4. Thermal damage obtained at the end of the temperature-controlled superficial laser irradiation for experiments (RGB images on the left of each figure) and simulations (right side of each figure) for the different controlling settings: (a) r = 6 mm, T_{th} = 55 °C, (b) r = 6 mm, T_{th} = 43 °C, (c) r = 2 mm, T_{th} = 55 °C, (d) r = 2 mm, T_{th} = 43 °C.

for the temperature regulation, i.e., the selection of the controlled zone, deeply affected the maximum temperature value (up to a difference of 33.4 °C considering the same T_{th} values, but different r). This highlights the importance of the implementation of a reliable predictive tool, able to estimate the maximum temperature values achievable with different settings of the control, to preplan the desired procedure [25].

A crucial factor for the optimal pre-planning of the controlled ablative treatment is the proper estimation of the final thermal injury. Several mathematical models have been proposed for the evaluation of the delivered thermal dose and the quantification of the tissue damage [26]. Here, we investigated the attained tissue damage ascribable to the different control settings (T_{th} and r) by employing the Arrhenius model and compared the results with the experimental outcomes.

Fig. 4 shows the damage on the *ex vivo* liver tissue after the superficial ablation procedure. Concerning the experimental assessment, the thermal lesions had quasi-circular shapes and the margins of ablation resulted visible for all the control cases except for the case of T_{th} = 43 °C and r = 2 mm. The maximum extent of tissue damage on the surface of the irradiated specimens (d_d) was calculated as the distance from the center of each lesion up to the most distant point where a laser-induced tissue change was observable. In the experiments, for r = 6 mm, d_d was approximately 5.3 mm in case of T_{th} = 55 °C, and 3.3 mm, for T_{th} = 43 °C. Moreover, for r = 2 mm and T_{th} = 55 °C, d_d was approximately 2.4 mm. The attained values were well predicted by the simulated thermal damage since for Ω = 0.6, the simulated d_d was 5.8 mm and 3.4 mm, at r = 6 mm, for T_{th} = 55 °C and 43 °C, respectively. Furthermore, for r = 6 mm and T_{th} = 55 °C, the predicted d_d was equal to 1.9 mm. The simulation also foresaw the absence of thermal damage in case of r = 2 mm and T_{th} = 43 °C, which was confirmed by the experimental analysis (Fig. 4.d).

Considering the attained temperature profiles, the two-dimensional spatial distribution, and the photothermal-induced damage, the combined simulated and experimental strategy showed its effectiveness. Particularly, it was possible to control the temperature at specified margins and to theoretically predict the outcome of the different control modalities. The main difference between the simulated and experimental values may be ascribed to the complexity of modeling the light interaction with soft tissue [19]. Indeed, turbid biological media are characterized by a multicompartmental structure with diverse optical properties [27]. Additionally, owing to the dependency of the optical and thermal properties on the attained temperature value , the pre-treatment description of the laser-induced tissue thermal behavior might result complicated [28]. Future studies should therefore focus on the consideration of temperature-dependent physical properties of the tissue in the model. Furthermore, to foster the applicability of the control strategy toward the *in vivo* scenario, the theoretical model should take into account also the influence of blood perfusion and metabolic heat, on the control outcome. The superficial LA setup considered in this study is a simplified model used for a preliminary and easily controlled temperature-feedback

Authorized licensed use limited to: Politecnico di Milano. Downloaded on July 29,2021 at 07:51:18 UTC from IEEE Xplore. Restrictions apply.

strategy. In the future, scenarios closer to the final clinical application should be considered.

IV. Conclusions

In this study, we propose a combined strategy based on a pre-planned and experimentally validated two-dimensional feedback control, to maintain the desired temperature within the selected tissue margins, during superficial LA. The pre-planning tool enabled a preliminary investigation of the influential control settings, i.e., r and $T_{th,}$ on the thermal outcome. The effectiveness of the theoretical model was assessed by comparison with the empirical results (e.g., a maximum difference of predicted and measured extension of superficial thermal damage of ~0.5 mm). The proposed strategy sets the basis for the development of a sensing platform for the optimal selection of the controlling settings for monitoring and regulation of the therapy outcome in contactless LA procedures.

Acknowledgment

This project has received funding from the European Research Council (ERC) under the European Union's Horizon 2020 research and innovation programme (Grant agreement No. 759159).

The authors would like to acknowledge Alexey Wolf and Alexander Dostovalov at the Institute of Automation and Electrometry of the SB RAS, Novosibirsk (Russia) for producing the fiber Bragg grating sensors mentioned in this work.

References

[1] E. Schena, P. Saccomandi, and Y. Fong, "Laser Ablation for Cancer: Past, Present and Future," *J. Funct. Biomater.*, vol. 8, no. 2, p. 19, Jun. 2017, doi: 10.3390/jfb8020019.

[2] K. Nagpal *et al.*, "Is minimally invasive surgery beneficial in the management of esophageal cancer? A meta-analysis," *Surg. Endosc.*, 2010, doi: 10.1007/s00464-009-0822-7.

[3] S. Lakhtakia and D. W. Seo, "Endoscopic ultrasonography-guided tumor ablation," *Digestive Endoscopy*. 2017, doi: 10.1111/den.12833.

[4] Z. Behrouzkia, Z. Joveini, B. Keshavarzi, N. Eyvazzadeh, and R. Z. Aghdam, "Hyperthermia: How can it be used?," *Oman Medical Journal*. 2016, doi: 10.5001/omj.2016.19.

[5] K. F. Chu and D. E. Dupuy, "Thermal ablation of tumours: biological mechanisms and advances in therapy," *Nat. Rev. Cancer*, vol. 14, no. 3, pp. 199–208, Mar. 2014, doi: 10.1038/nrc3672.

[6] S. Asadi, L. Bianchi, M. De Landro, S. Korganbayev, E. Schena, and P. Saccomandi, "Laser-induced optothermal response of gold nanoparticles: From a physical viewpoint to cancer treatment application," *J. Biophotonics*, vol. 14, no. 2, Feb. 2021, doi: 10.1002/jbio.202000161.

[7] S. J. Payne, T. Peng, and D. P. O'Neill, "Mathematical modeling of thermal ablation," *Critical Reviews in Biomedical Engineering*. 2010, doi: 10.1615/CritRevBiomedEng.v38.i1.30.

[8] S. Korganbayev *et al.*, "Closed-Loop Temperature Control Based on Fiber Bragg Grating Sensors for Laser Ablation of Hepatic Tissue," *Sensors*, vol. 20, no. 22, p. 6496, Nov. 2020, doi: 10.3390/s20226496.

[9] S. Korganbayev, R. Pini, A. Orrico, A. Wolf, A. Dostovalov, and P. Saccomandi, "Towards temperature-controlled laser ablation based on fiber Bragg grating array temperature measurements," in *2020 IEEE International Workshop on Metrology for Industry 4.0 and IoT, MetroInd 4.0 and IoT 2020 - Proceedings*, 2020, doi: 10.1109/MetroInd4.0IoT48571.2020.9138171.

[10] J.-T. Lin, Y.-S. Chiang, G.-H. Lin, H. Lee, and H.-W. Liu, "In Vitro Photothermal Destruction of Cancer Cells Using Gold Nanorods and Pulsed-Train Near-Infrared Laser," *J. Nanomater.*, vol. 2012, pp. 1–6, 2012, doi: 10.1155/2012/861385.

[11] J. Lin, Y. Hong, and C. Chang, "Selective cancer therapy via IR-laser-excited gold nanorods," vol. 7562, pp. 1–5, 2010, doi: 10.1117/12.841348.

[12] P. H. Mollert, L. Lindbergt, P. H. Henriksson, and K. Tranberg, "Temperature control and light penetration in a feedback interstitial laser thermotherapy system," vol. 12, no. 1, pp. 49–63, 1996.

[13] K. Ivarsson, J. Olsrud, and C. Sturesson, "Feedback Interstitial Diode Laser (805 nm) Thermotherapy System : Ex Vivo Evaluation and Mathematical Modeling With One and Four-Fibers," vol. 96, no. September 1997, pp. 86–96, 1998.

[14] L. Bianchi *et al.*, "Fiber Bragg Grating Sensors for Thermometry during Gold Nanorods-mediated Photothermal Therapy in Tumor Model," in *2020 IEEE Sensors*, Oct. 2020, pp. 1–4, doi: 10.1109/SENSORS47125.2020.9278580.

[15] F. Morra *et al.*, "Spatially resolved thermometry during laser ablation in tissues: Distributed and quasi-distributed fiber optic-based sensing," *Opt. Fiber Technol.*, vol. 58, p. 102295, Sep. 2020, doi: 10.1016/j.yofte.2020.102295.

[16] J. P. Ritz, A. Roggan, C. Isbert, G. Mller, H. J. Buhr, and C. T. Germer, "Optical properties of native and coagulated porcine liver tissue between 400 and 2400 nm," *Lasers Surg. Med.*, vol. 29, no. 3, pp. 205–212, 2001, doi: 10.1002/lsm.1134.

[17] P. Saccomandi *et al.*, "Theoretical Analysis and Experimental Evaluation of Laser-Induced Interstitial Thermotherapy in Ex Vivo Porcine Pancreas," *IEEE Trans. Biomed. Eng.*, vol. 59, no. 10, pp. 2958–2964, Oct. 2012, doi: 10.1109/TBME.2012.2210895.

[18] A. Ishimaru, "Diffusion of light in turbid material," *Appl. Opt.*, vol. 28, no. 12, p. 2210, Jun. 1989, doi: 10.1364/AO.28.002210.

[19] T. H. Nguyen, S. Park, K. K. Hlaing, and H. W. Kang, "Temperature feedback-controlled photothermal treatment with diffusing applicator: theoretical and experimental evaluations," *Biomed. Opt. Express*, vol. 7, no. 5, p. 1932, May 2016, doi: 10.1364/BOE.7.001932.

[20] Harry H. Pennes, "Analysis of tissue and arterial blood temperatures in the resting human forearm," *J. Appl. Physiol.*, vol. I, 1948.

[21] S. Singh and R. Repaka, "Quantification of Thermal Injury to the Healthy Tissue Due to Imperfect Electrode Placements During Radiofrequency Ablation of Breast Tumor," *J. Eng. Sci. Med. Diagnostics Ther.*, vol. 1, no. 1, pp. 1–10, 2018, doi: 10.1115/1.4038237.

[22] Markolf H. Niemz, *Laser-tissue Iteractions: Fundamentals and Applications*. Springer-Verlag, 2004.

[23] F. C. HENRIQUES, "Studies of thermal injury; the predictability and the significance of thermally induced rate processes leading to irreversible epidermal injury," *Arch. Pathol.*, 1947.

[24] G. Zorbas and T. Samaras, "Simulation of radiofrequency ablation in real human anatomy," *Int. J. Hyperth.*, 2014, doi: 10.3109/02656736.2014.968639.

[25] L. Bianchi, S. Korganbayev, A. Orrico, M. De Landro, and P. Saccomandi, "Quasi-distributed fiber optic sensor-based control system for interstitial laser ablation of tissue: theoretical and experimental investigations," *Biomed. Opt. Express*, vol. 12, no. 5, p. 2841, May 2021, doi: 10.1364/BOE.419541.

[26] J. Pearce, "Mathematical models of laser-induced tissue thermal damage," *Int. J. Hyperth.*, vol. 27, no. 8, pp. 741–750, Dec. 2011, doi: 10.3109/02656736.2011.580822.

[27] A. J. Welch and M. J. C. Van Gemert, *Optical-Thermal Response of Laser-Irradiated Tissue*. Dordrecht: Springer Netherlands, 2011.

[28] S. Kim and S. Jeong, "Effects of temperature-dependent optical properties on the fluence rate and temperature of biological tissue during low-level laser therapy," *Lasers Med. Sci.*, 2014, doi: 10.1007/s10103-013-1376-4.

Authorized licensed use limited to: Politecnico di Milano. Downloaded on July 29,2021 at 07:51:18 UTC from IEEE Xplore. Restrictions apply.